

Automatic vegetation identification in Google Earth images using a convolutional neural network: A case study for Japanese bamboo forests

Shuntaro Watanabe¹, Kazuaki Sumi², Takeshi Ise^{1,3}

1. Field Science Education and Research Center (FSERC), Kyoto University, Kitashirakawaoiwake-cho, Sakyo-ku, Kyoto 606-8502, Japan
2. Graduate School of Agriculture, Kyoto University, Kitashirakawaoiwake-cho, Sakyo-ku, Kyoto 606-8502, Japan
3. PRESTO, Japan Science and Technology Agency, 7 Goban-cho, Chiyoda-ku, Tokyo 102-0076, Japan

Running head: Vegetation identification using deep learning

Author for correspondence: SW

E-mail: sh.watanabe1006@gmail.com (SW)

1 **ABSTRACT**

2 Classifying and mapping vegetation are very important tasks in environmental science
3 and natural resource management. However, these tasks are not easy because
4 conventional methods such as field surveys are highly labor intensive. Automatic
5 identification of target objects from visual data is one of the most promising ways to
6 reduce the costs for vegetation mapping. Although deep learning has become a new
7 solution for image recognition and classification recently, in general, detection of
8 ambiguous objects such as vegetation still is considered difficult. In this paper, we
9 investigated the potential for adapting the chopped picture method, a recently described
10 protocol for deep learning, to detect plant communities in Google Earth images. We
11 selected bamboo forests as the target. We obtained Google Earth images from three
12 regions in Japan. By applying the deep convolutional neural network, the model
13 successfully learned the features of bamboo forests in Google Earth images, and the
14 best trained model correctly detected 97% of the targets. Our results show that
15 identification accuracy strongly depends on the image resolution and the quality of
16 training data. Our results also highlight that deep learning and the chopped picture
17 method can potentially become a powerful tool for high accuracy automated detection
18 and mapping of vegetation.

19

20 **Key Words**

21 Deep learning, Convolutional neural network, Vegetation mapping, Google Earth
22 imagery

23

24 INTRODUCTION

25 Classifying and mapping vegetation are essential tasks for environmental science
26 research and natural resource management¹. Traditional methods (e.g., field surveys,
27 literature reviews, manual interpretation of aerial photographs), however, are not
28 effective for acquiring vegetation data because they are labor intensive and often
29 economically expensive. The technology of remote sensing offers a practical and
30 economical means to acquire information on vegetation cover, especially over large
31 areas². Because of its systematic observations at various scales, remote sensing
32 technology potentially can enable classification and mapping of vegetation at high
33 temporal resolutions.

34 Detection of discriminating visual features is one of the most important steps in
35 almost any computer vision problem, including in the field of remote sensing. Since
36 conventional methods such as support vector machines³ require hand-designed, time-
37 consuming feature extraction, substantial efforts have been dedicated to development of
38 methods for the automatic extraction of features. Recently, deep learning has become a
39 new solution for image recognition and classification because this new method does not
40 require the manual extraction of features.

41 Deep learning^{4,5} is one type of machine learning technique that uses algorithms
42 inspired by the structure and function of the brain called artificial neural networks. Deep
43 learning involves the learning of features and classifiers simultaneously, and it uses
44 training data to categorize image content without a priori specification of image
45 features. Among all deep learning-based networks, the convolutional neural network
46 (CNN) is the most popular for learning visual features in computer vision applications
47 including remote sensing. Recent research has shown that CNN is effective for diverse

48 applications⁴⁻⁷. Given its success, deep learning has been used intensively in several
49 distinct tasks for different academic and industrial fields including plant science. Recent
50 research has shown that the deep learning technique can successfully detect plant
51 disease, correctly classify the plant specimens in a herbarium⁸⁻¹⁰

52 Deep learning is a promising technology also in the field of remote sensing^{11,12}.
53 Recently, Guirado et al., (2017)¹³ demonstrated that the deep learning technique
54 successfully detect plant species of conservation concern and it provides better results
55 than the conventional object detection methods. However, application of deep learning
56 to vegetation mapping are not sufficient yet because vegetation in the aerial image often
57 shows ambiguous and amorphous shape, and automatic object identification including
58 deep learning tends not to work well on such objects.

59 Recently, Ise et al., (2018)¹⁴ developed a method to extract relevant
60 characteristics from ambiguous and amorphous objects. This method dissects the
61 images into numerous small squares and efficiently produces the training images. By
62 using this method, Ise et al. (2018)¹⁴ correctly classified three moss species and “non-
63 moss” objects in test images with an accuracy of more than 90%.

64 In this paper, we investigated the potential for adapting a deep learning model
65 and the chopped picture method to automatic vegetation detection in Google Earth
66 images, and bamboo forests were used as the target. In recent years, bamboo has
67 become invasive in Japan. The bamboo species moso (*Phyllostachys edulis*) and
68 madake (*P. bambusoides* Siebold) are the two main types of exotic bamboo. Since the
69 1970s, the bamboo industry in Japan had declined as a result of cheaper bamboo
70 imports and heavy labor costs¹⁵. Consequently, many bamboo plantations were left
71 unmanaged, which led to the eventual invasion of adjacent native vegetation¹⁶⁻¹⁸.

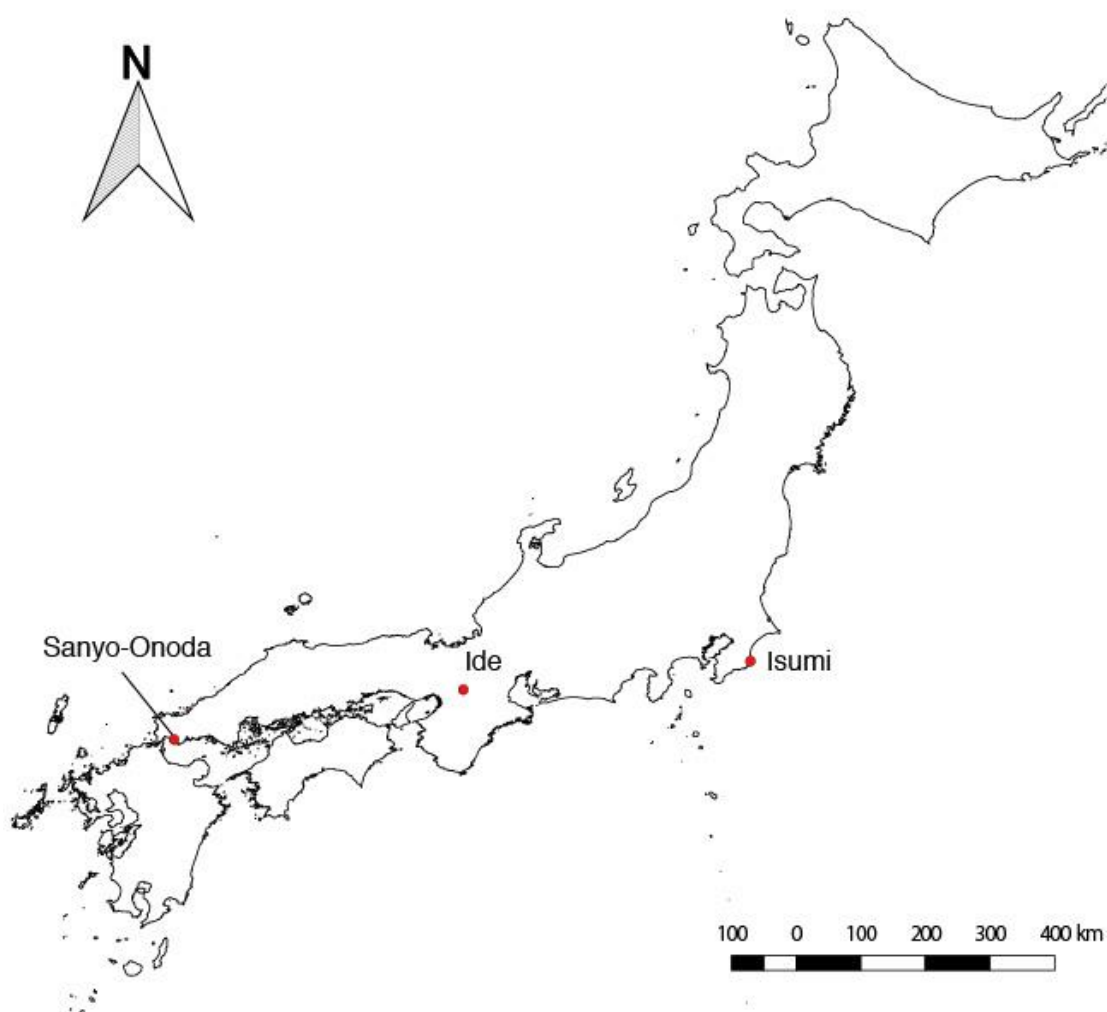
72 In this study, we specifically addressed the following questions: 1) how does the
73 resolution of images affect the accuracy of detection; 2) how does the chopping size of
74 training images affect the accuracy of detection; and 3) can a model that learned in one
75 geographical location work well for a different location?

76

77 **MATERIALS AND METHODS**

78 **Target area and image acquisition**

79 In this study, we chose three regions (Sanyo-Onoda, Ide, and Isumi) in Japan to conduct
80 the analyses (Figure 1). We used Google Earth as the source of imagery. From a given
81 sampling location, we obtained the images at zoom levels of 1/500 (~0.13 m/pixel
82 spatial resolution), 1/1000 (~0.26 m/pixel spatial resolution), and 1/2500 (~0.65 m/pixel
83 spatial resolution).



84

85 FIGURE 1 Target regions of this research.

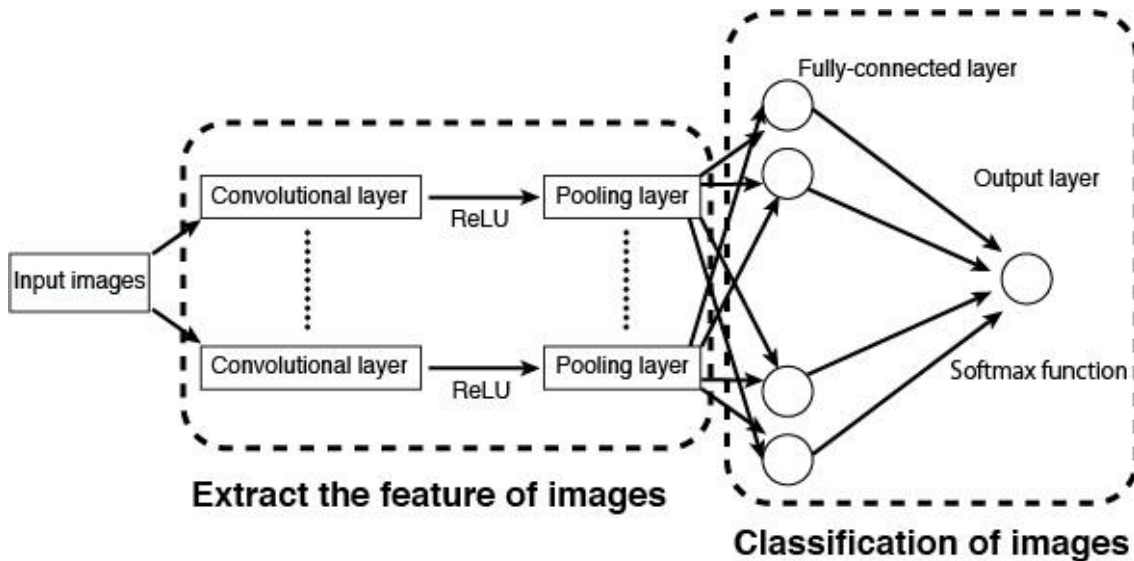
86

87 **Methods and background concepts for the neural networks**

88 In this study, we employed convolutional neural networks (CNN; Figure 2). A CNN is a

89 special type of feedforward neural network that consists of a convolutional layer and

90 pooling layer.



91

92 FIGURE 2 Schematic diagram of the convolutional neural networks.

93

94 A feedforward neural network is an artificial neural network wherein
95 connections between the nodes do not form a cycle. These networks, which conduct
96 modeling similar to the neuron activity in the brain, are generally presented as systems
97 of interconnected processing units (artificial neurons) that can compute values from
98 inputs leading to an output that may be used on further units. Artificial neurons are
99 basically processing units that compute some operation over several input variables and,
100 usually, have one output calculated through the activation function. Typically, an
101 artificial neuron has a weight w_i that represents the degree of connection between
102 artificial neurons, some input variables x_i , and a threshold vector b . Mathematically,
103 the total input and output of artificial neurons can be described as follows:

104

$$105 \quad u = \sum_i w_i x_i \quad (1)$$

106

107 $z = f(u + b) = f(\sum_i w_i x_i + b)$ (2)

108

109 where u , z , x , w , and b represent the total input, output, input variables, weights, and
110 bias, respectively. $f(\cdot)$ denotes an activation function; a nonlinear function such as a
111 sigmoid, hyperbolic, or rectified linear function is provided in $f(\cdot)$. We employed a
112 rectified linear function as the activation function, and this function is referred to as the
113 Rectified Linear Unit (ReLU). The definition of ReLU is shown in the following
114 equation:

115

116 $f(u) = \max\{0, u\} = \begin{cases} u & (u > 0) \\ 0 & (u \leq 0) \end{cases}$ (3)

117

118 As mentioned above, a CNN is a special type of feedforward neural network that
119 is usually used in image classification and identification. A CNN consists of a
120 convolutional layer and pooling layer. The convolutional layer plays a role in capturing
121 the features from the images. In this process, a fixed-sized window runs over the image
122 and extracts the patterns of shades of colors in the image. After each convolutional
123 layer, there are pooling layers that are created in order to reduce the variance of
124 features, which is accomplished by computing some operation of a particular feature
125 over a region of the image.

126 The pooling layer has the function of reducing the position sensitivity of the
127 feature that is extracted at the convolution layer so that the output amount of the pooling
128 layer does not change even when the position of the feature amount extracted by the
129 convolution layer is shifted within the image. Two operations may be realized on the

130 pooling layers, namely, max or average operations, in which the maximum or mean
131 value is selected over the feature region, respectively. This process ensures that the
132 same results can be obtained, even when image features have small translations or
133 rotations, and this is very important for object classification and detection. Thus, the
134 pooling layer is responsible for sampling the output of the convolutional one and
135 preserving the spatial location of the image, as well as selecting the most useful features
136 for the next layers.

137 After several convolutional and pooling layers, there are fully connected ones,
138 which take all neurons in the previous layer and connect them to every single neuron in
139 its layer.

140 Finally, following all of the convolution, pooling, and fully connected layers, a
141 classifier layer may be used to calculate the class probability of each instance. We
142 employed the softmax function in this layer. The softmax function calculates the
143 probabilities of each target class over all possible target classes. The softmax function is
144 written as follows:

145

$$146 \quad y_k = \text{softmax}_k(u_1, u_2, \dots, u_K) = \frac{e^{u_k}}{\sum_{j=1}^K e^{u_j}} \quad (4)$$

147

148 where k represents the number of the output unit and u represents input variables.

149 In order to evaluate the performance of the network, a loss function needs to be
150 defined. The loss function evaluates how well the network models the training dataset.
151 The goal of the training is to minimize the error of the loss function. Eq. (5) presents the
152 cross entropy of the softmax function that was employed in this study:

153

154
$$E = -\sum_{n=1}^N \sum_{k=1}^K t_{n,k} \log y_k \tag{5}$$

155

156 where t is the vector for the training data, K represents the possible class, and N

157 represents the total number of instances.

158

159 Approach

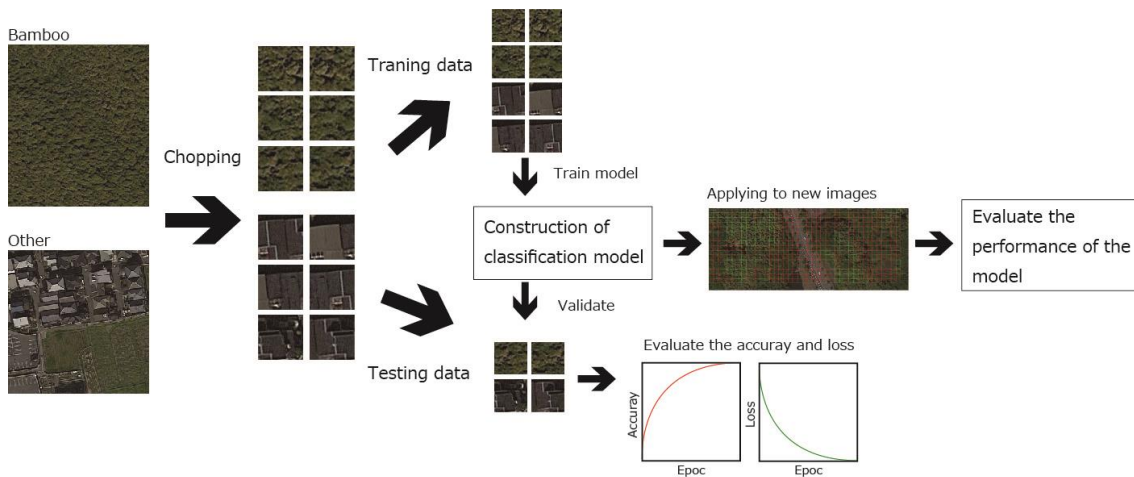
160 A schematic diagram of our approach is shown in Figure 3. We prepared the training

161 data by using the chopped picture method¹⁴. First, in this method, we collected the

162 images that were (1) nearly 100% covered by bamboo and (2) not covered by bamboo.

163 Next, we “chopped” this picture into small squares with 50% overlap both vertically

164 and horizontally.



165

166 FIGURE 3 Schematic diagram of the research approach. This figure was

167 generated using data from Google Earth image (Image data: ©2018

168 CNES/Airbus & Digital Globe).

169

170 We made a model for image classification from a deep CNN for the bamboo
171 forest detection. As opposed to traditional approaches of training classifiers with hand-
172 designed feature extraction, the CNN learns the feature hierarchy from pixels to
173 classifiers and trains layers jointly. We used the final layer of the CNN model for
174 detecting the bamboo coverage from Google Earth images. To make a model for object
175 identification, we used the deep learning framework of NVIDIA DIGITS¹⁹. We used
176 75% of the obtained images as training data and the remaining 25% as validation data.
177 We used the LeNet network model²⁰. The model parameters implemented in this study
178 included the number of training epochs (30), learning rate (0.01), train batch size (64),
179 and validation batch size (32).

180

181 **Evaluation of the learning accuracy**

182 Validation of the model in each learning epoch was conducted by using the accuracy
183 and loss function obtained from cross validation images. The accuracy indicates how
184 accurately the model can classify the validation images. Loss represents the inaccuracy
185 of the prediction of the model. If model learning is successful, loss (val) is low and
186 accuracy is high. However, when loss (val) becomes high during learning, this indicates
187 that over fitting is occurring.

188

189 **Evaluation of the model performance**

190 We obtained 10 new images, which were uniformly covered by bamboo forest or
191 objects other than bamboo forest, from each study site. Next, we re-sized the images by
192 using the chopped picture method. Third, we randomly sampled 500 images from the

193 re-sized images. Finally, we applied the model to the sampled images and evaluated the
194 classification accuracy. To evaluate the performance of the model, we classified the
195 classification results into the following four categories: true positive (*TP*), false positive
196 (*FP*), false negative (*FN*), and true negative (*TN*). Next, we calculated the classification
197 accuracy, recall rate, and precision rate by using the following equations:

198

$$199 \text{ Classification accuracy} = (TP + TN)/(TP + TN + FP + FN) \quad (6)$$

200

$$201 \text{ Recall rate} = TP/(TP + FN) \quad (7)$$

202

$$203 \text{ Precision rate} = TP/(TP + FP) \quad (8)$$

204

205 **Testing the effects of image resolution on the classification accuracy**

206 To quantify the effects of image resolution on the accuracy of detection, we obtained
207 images at a zoom level of 1/500 (~0.13 m/pixel spatial resolution), 1/1000 (~0.26
208 m/pixel spatial resolution), and 1/2500 (~0.65 m/pixel spatial resolution) from each
209 study site. Next, we applied the chopped picture method. To adjust the spatial extent of
210 each chopped image, we chopped 56 pixels for the 1/500 level, 28 pixels for the 1/1000
211 level, and 14 pixels for the 1/2500 level. After constructing the model, we applied the
212 model to the new images and calculated the classification accuracy, recall rate, and
213 precision rate.

214

215 **Testing the effects of chopping grid size on the classification accuracy**

216 To quantify the effects of the spatial extent of the chopping grid on the accuracy of
217 detection, we chopped the 1/500 images at each study site for three types of pixel sizes
218 (84, 56, 28). After constructing the model, we applied the model to new images and
219 calculated the classification accuracy, recall rate, and precision rate.

220

221 **Transferability test**

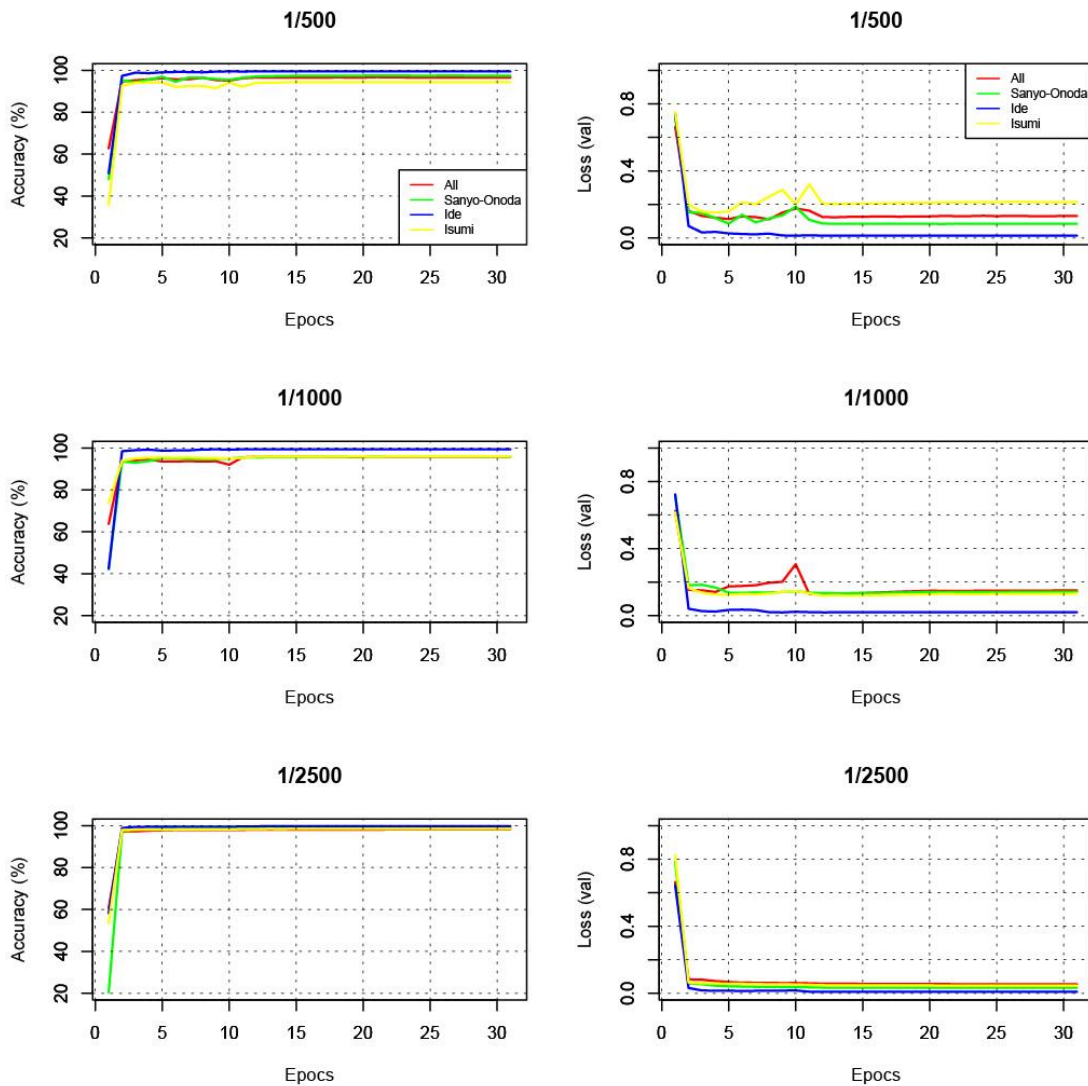
222 Given the large amount of variation in the visual appearance of bamboo forest across
223 different cities, it is of interest to study to what extent a model learned on one
224 geographical location can be applied to a different geographical location. As such, we
225 performed experiments in which we trained a model for one (or more) cities, and then,
226 we applied the model to a different set of cities. Performance of the model was
227 evaluated by the classification accuracy, recall rate, and precision rate.

228

229 **RESULTS**

230 **Fluctuation of accuracy and loss during the learning epochs**

231 The accuracy for classifying the validation data of the final layer ranged from 94% to
232 99%. Loss values for the validation data ranged from 0.008 to 0.214 (Figure 4). Values
233 of accuracy increased and loss decreased following the learning epochs (Figure 4).
234 These results suggest the all of the models were not overfit to the datasets and
235 successfully learned the features of chopped pictures.



236

237 FIGURE 4 Accuracy and loss (val) of the model at each learning epoch.

238

239 **Effects of image resolution on the classification accuracy**

240 The classification accuracy ranged from 76% to 97% (Figure 5a). The recall rate and

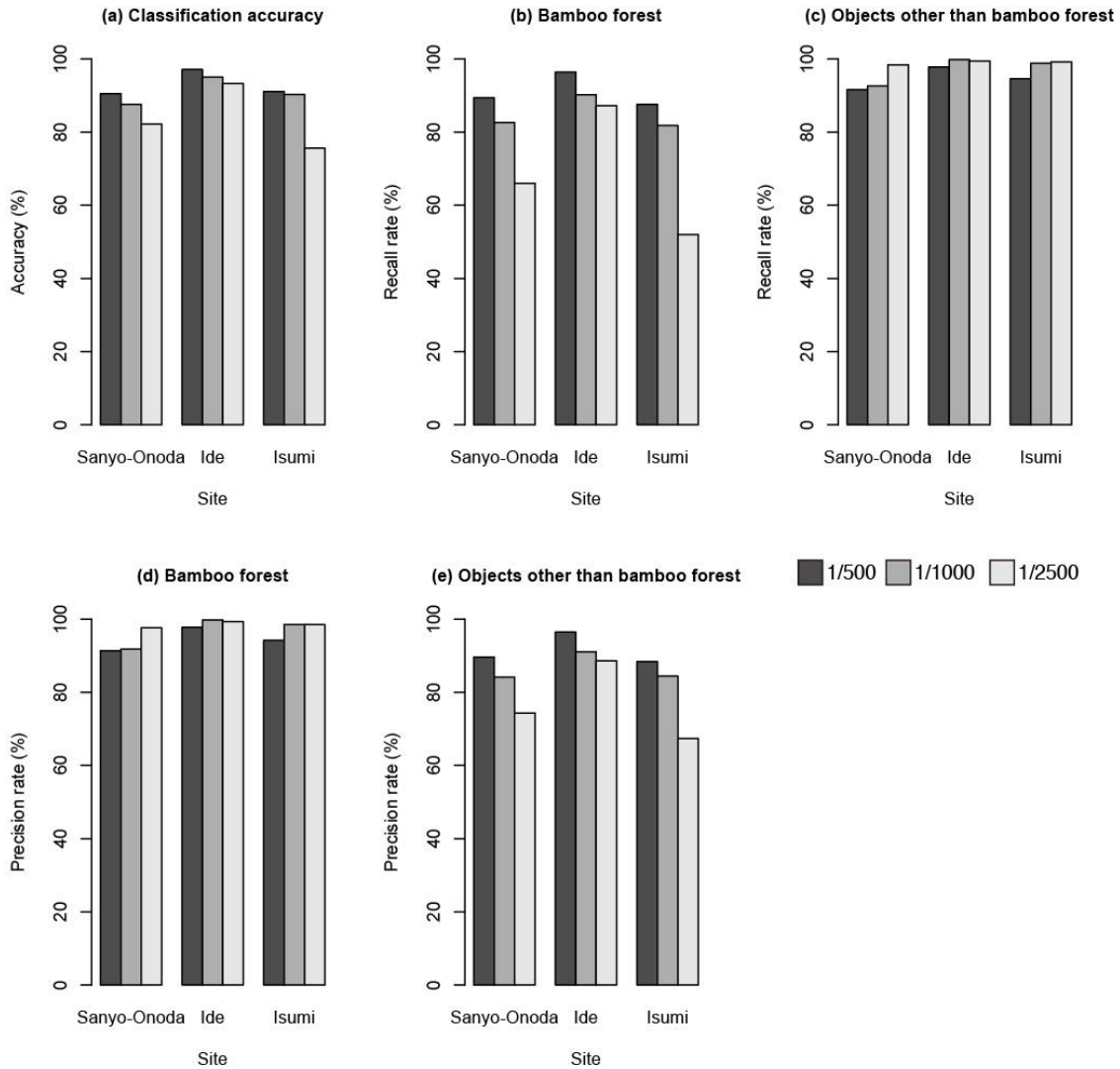
241 precision rate for bamboo forest ranged 52% to 96% and 91% to 99%, respectively

242 (Figure 5b, d). The recall rate and precision rate for objects other than bamboo forest

243 ranged from 92% to 99% and 67% to 96%, respectively (Figure 5c, e). The recall rate

244 for bamboo forest declined following the decline in the image resolution, and it declined

245 dramatically when we used the 1/2500 level (~0.65 m/pixel spatial resolution) (Figure
246 5a).



247

248 **FIGURE 5** Sensitivity of the image scale versus the test accuracy.

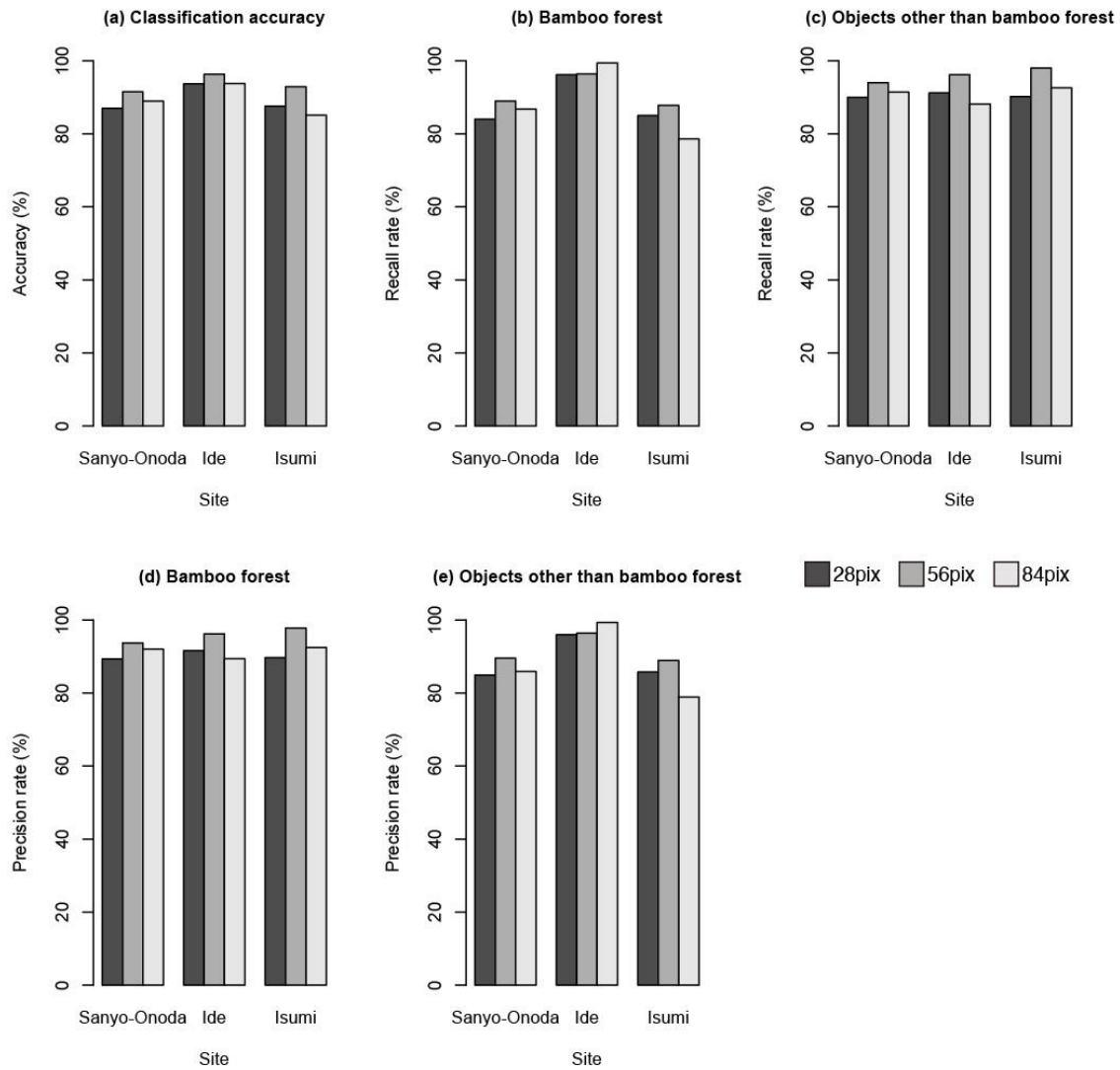
249

250 **Effects of chopping grid size on the classification accuracy**

251 The classification accuracy ranged from 85% to 96% (Figure 6a). The recall rate and
252 precision rate for bamboo forest ranged from 79% to 99% and 89% to 98%, respectively

253 (Figure 6b, d). The recall rate and precision rate for objects other than bamboo forest

254 ranged from 88% to 98% and 79% to 99%, respectively (Figure 6c, e). The
255 intermediate-sized images (56 pixel) showed the highest classification accuracy at all
256 sites (Figure 6a). An example of a classification image is shown in Figure 7.



257

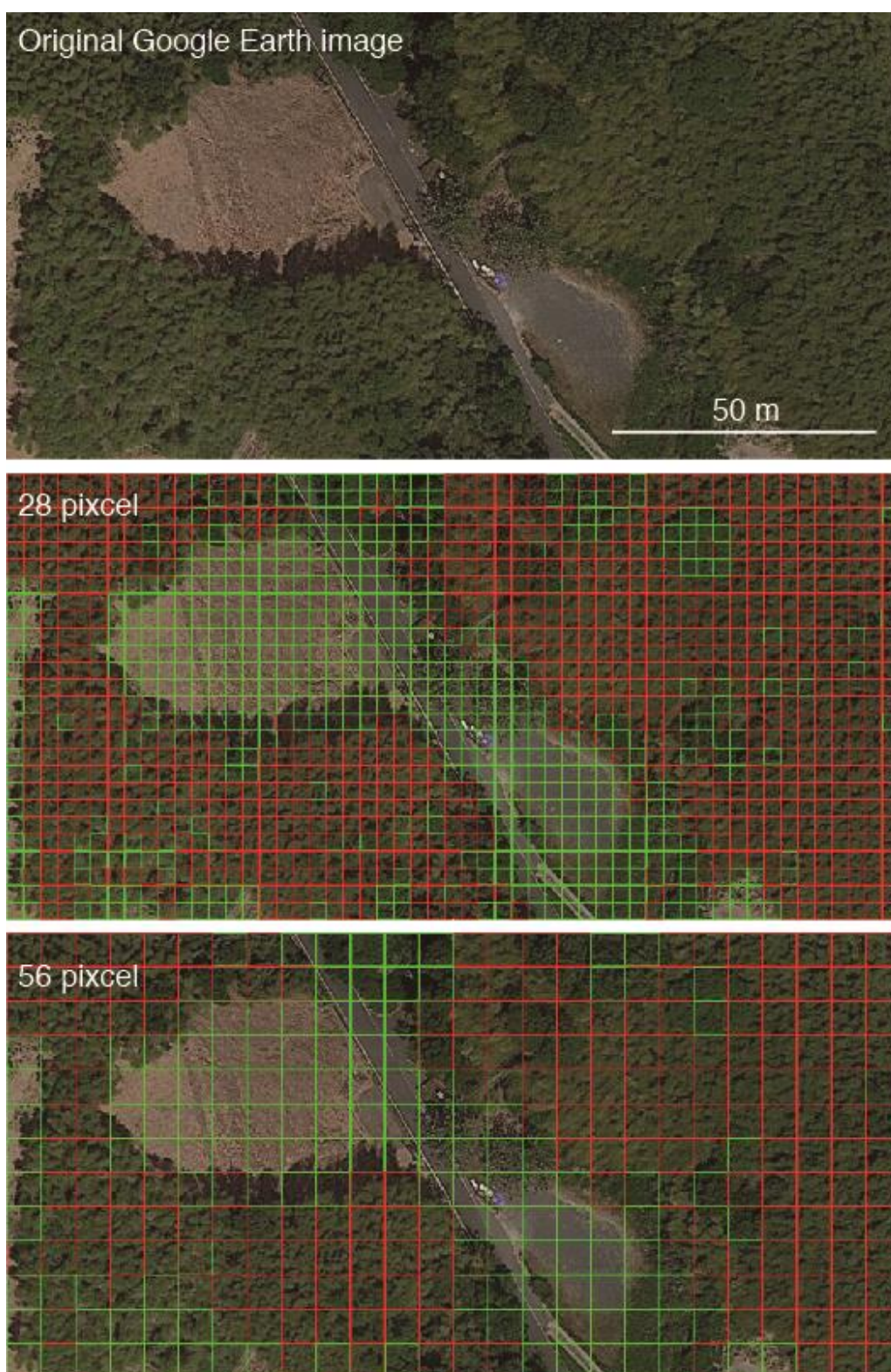
258 FIGURE 6 Sensitivity of the pixel size versus the test accuracy.

259

260

261

262



263

264 FIGURE 7 Example of a classification image. Bamboo forests are highlighted by

265 red, and objects other than bamboo are highlighted by green. This figure was

266 generated using data from Google Earth image (Image data: ©2018

267 CNES/Airbus & Digital Globe).

268

269 **Transferability and classification performance**

270 In general, performance was poor when training on samples from a given city and

271 testing on samples from a different city (Figure 8a). When the model that was trained by

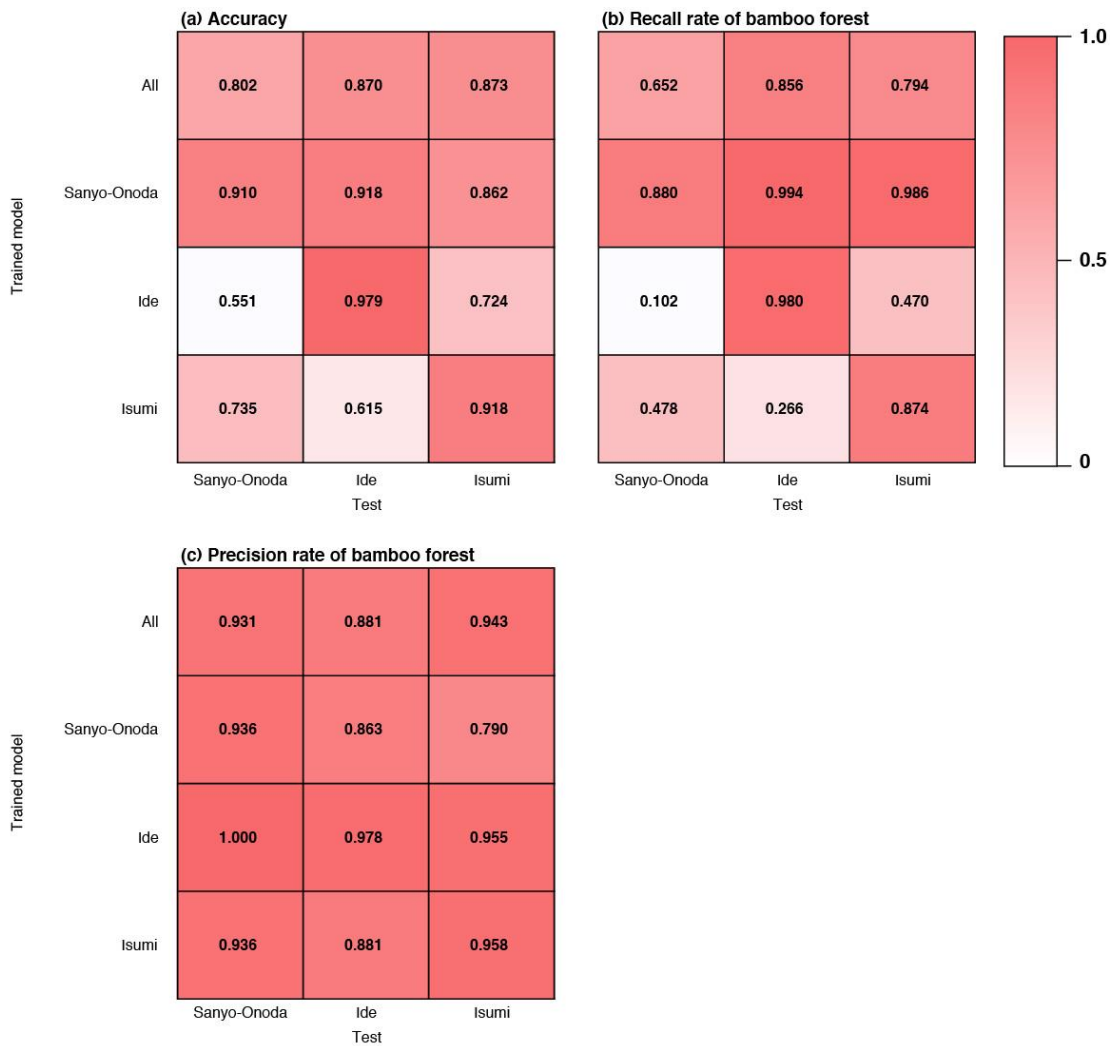
272 the images of Isumi city was applied to the other cities, the recall rate was the worst

273 (Figure 8b). Conversely, the model that was trained by the images of Sanyo city showed

274 the highest recall rate (Figure 8b). We noticed that a more diverse set (all) did not yield

275 a better performance when applied at different locations than the models trained on

276 individual cities (Figure 8).



277

278 FIGURE 8 Transferability of the models learned at one location and applied at
 279 another.

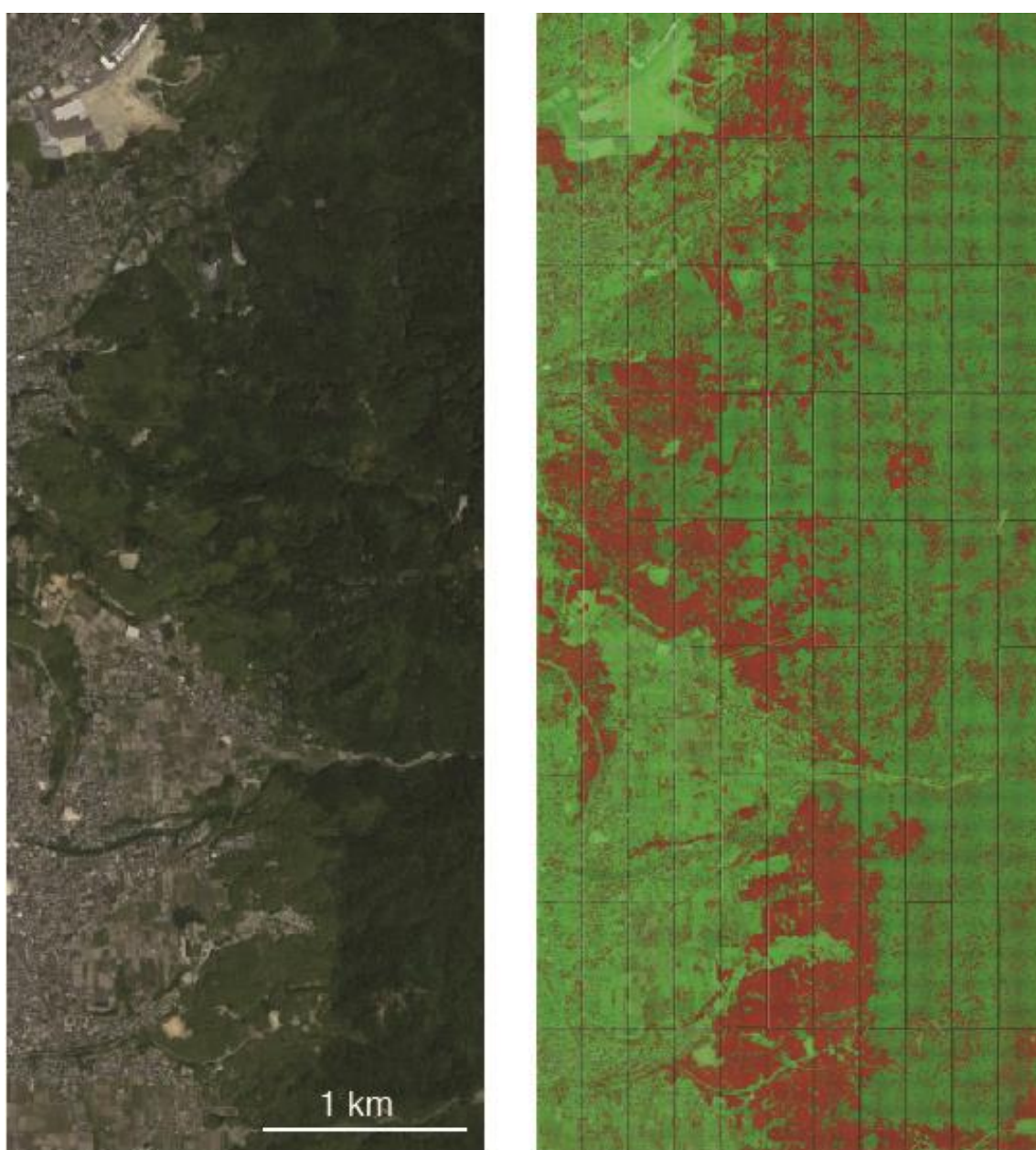
280

281 DISCUSSION

282 In this paper, we demonstrated that the chopped picture method and CNN could
 283 accurately detect bamboo forest in Google Earth imagery (see Figure 7). Recent
 284 research has shown that the deep learning technique is applicable to plant science
 285 research^{8-11, 21,22}; however, applications of DA in plant science have been mainly
 286 restricted to photographs taken indoors, and applications to plants in the aerial

287 photographs are still limited¹¹. To the best of our knowledge, this is the first study to
288 successfully identify plant communities automatically from Google Earth imagery.

289 Classifying vegetation from remote sensing images generally suffers from
290 several problems, e.g., it can be difficult to establish a specific pattern for each species,
291 given the high intraclass variance, and also to distinguish between different species,
292 given the interclass similarity of distinct species^{12, 23}. So far, it is generally been difficult
293 to detect ambiguous objects such as vegetation, but our results showed good
294 performance during the detection of bamboo forest from Google Earth images by using
295 the chopped picture method even though we employed the most classical CNN (LeNet).
296 Our results highlight that the chopped picture method and CNN would be a powerful
297 method for high accuracy automated bamboo forest detection and vegetation mapping
298 (see Figure 9).



299

300 FIGURE 9 Example of applying the model to the wide area of Ide city. The left
301 image is the original Google Earth image, and the right image shows the results
302 of bamboo forest detection. Bamboo forests are highlighted by red, and objects
303 other than bamboo are highlighted by green. This figure was generated using
304 data from Google Earth image (Image data: ©2018 CNES/Airbus & Digital
305 Globe).

306

307

308 **Effects of image resolution on the classification accuracy**

309 Our results indicate that the image resolution strongly affects the identification accuracy
310 (Figure 4). As the resolution rate decreased, performance of the model also declined
311 (Figure 4).

312 Especially in the 1/2500 imagery, the recall rate for bamboo forest of Sanyo-
313 Onoda and Isumi city declined to 53% and 64%, respectively (Figure 4b). In contrast,
314 the precision rate for bamboo forest increased as the resolution decreased (Figure 4d).
315 This result means that as the resolution decreases, the model overlooks many bamboo
316 forests; thus, when the image resolution is low, it is difficult to learn the features of the
317 object. This result also suggests that in the deep learning model, misidentification due to
318 false negatives is more likely to occur than misidentification due to false positive as the
319 image resolution declines.

320

321 **Effects of chopping grid size on the classification accuracy**

322 Our results indicate that the chopping grid size also affects the performance of the
323 model. The classification accuracy was the highest at the medium pixel size (56 × 56
324 pixels; Figure 5a). In contrast to the effects of image resolution, the recall rate and
325 precision rate for bamboo forest was also the highest at the medium pixel size except for
326 the recall rate at Ide city (Figure 5b, d).

327 This result means that if the grid size is inappropriate, both false positives and false
328 negatives will increase.

329 Increases of the chopping grid size will cause an increase in the number of
330 chopped pictures in which objects other than bamboo and bamboo are mixed. In this
331 paper, because we evaluated the performance of the model by using images that were
332 uniformly covered by bamboo forest or objects other than bamboo forest, the effects of
333 imagery consisting of mixed objects on the classification accuracy could not be
334 evaluated. Evaluation of the classification accuracy for such images will take place in
335 future research.

336

337 **Transferability among the models**

338 Results for the transferability tests showed that transferability was generally poor and
339 suggest that the spatial extent of acquisition of training data strongly influences the
340 classification accuracy (Figure 8). The model trained by Sanyo-Onoda city images
341 yielded high recall rates for the images taken at all of the study sites, but the precision
342 rate was lower than that of the other models (Figure 8b, c). This means that the model
343 trained by Sanyo-Onoda city images tends to make false positive mistakes.
344 Interestingly, transferability was not found to be related to the distance among the study
345 sites (Figure 8). This result indicates that classification accuracy across the model
346 reflects the conditions at the local scale such as the climate at the time when the image
347 was taken. Additionally, even when we applied a model that learned from all training
348 images (all), the performance of the model was not as good as when the training data
349 were obtained within the same city. The same tendencies have been reported in studies
350 that classified land use by using deep learning²⁴. This may suggest that increasing the
351 number of training data may also lead to a decrease in the identification accuracy, and it
352 may be difficult to construct an identification model applicable to a broad area.

353

354 **Conclusions and future directions**

355 Our results show that the deep learning model presented here can detect bamboo forest
356 from Google Earth images accurately. Our results also suggest that deep learning and
357 the chopped picture method would be a powerful tool for high accuracy automated
358 vegetation mapping and may offer great potential for reducing the effort and costs
359 required for vegetation mapping as well as improving the current status of monitoring
360 the distribution of bamboo. Recently, bamboo expansion has become an important
361 problem in Japan because of its invasiveness¹⁷. While some research has analyzed the
362 bamboo forest distribution probability on a national scale^{25, 26}, monitoring of bamboo
363 expansion is still a challenging problem because of labor requirements. Our approach
364 could potentially lead to the creation of a semi or even fully automated system for the
365 monitoring of bamboo expansion.

366 Our results also suggest that the identification accuracy depends on the image
367 resolution and chopping grid size. Especially, the spatial resolution of training data
368 strongly affects the model performance. Generally, satellite-based remote sensing has
369 been widely studied and applied but suffers from insufficient information due to low
370 resolution images or inaccurate information due to local weather conditions²⁷. Our
371 results also show that the performance of the model can be greatly influenced by the
372 spatial extent of the acquired training data and a model learned on one geographical
373 location is difficult to apply to a different geographical location. It remains a future task
374 to develop a model that can be applied over a wide spatial scale.

375

376 **ACKNOWLEDGEMENTS**

377 This work was supported by JST PRESTO, Japan (Grant No. JPMJPR15O1).

378

379 **Author Contributions**

380 S. W designed the research based on discussion with T. I. S. W and K. S

381 conducted research. S. W and T. I wrote the manuscript.

382

383 **Competing interests**

384 The authors declare no competing interests.

385

386

387

388 REFERENCES

- 389 1. Franklin, J. *Mapping Species Distributions: Spatial Inference and Prediction*.
390 (Cambridge University Press, 2009).
- 391 2. Xie, Y., Sha, Z., & Yu, M. Remote sensing imagery in vegetation mapping: a review.
392 *Journal of Plant Ecology*, 1, 9–23. doi: 10.1093/jpe/rtm005 (2008).
- 393 3. Hearst, M. A., Dumais, S. T., Osuna, E., Platt, J., & Schölkopf, B. Support vector
394 machines. *IEEE Intelligent Systems and their Applications*, 13, 18–28. doi:
395 10.1109/5254.708428 (1998).
- 396 4. Bengio, Y. Learning deep architectures for AI. *Foundations and Trends in Machine
397 Learning*, 2, 1–127 (2009).
- 398 5. Goodfellow, I., Bengio, Y. & Courville, A. *Deep Learning* (MIT press, 2016)
- 399 6. Karpathy, A., Toderici, G., Shetty, S., Leung, T., Sukthankar, R., & Fei-Fei, L.
400 Large-scale video classification with convolutional neural networks. *Proceedings of
401 the IEEE Conference on Computer Vision and Pattern Recognition* (Columbus),
402 1725–1732 (2014).
- 403 7. Yosinski, J., Clune, J., Bengio, Y., & Lipson, H. How transferable are features in
404 deep neural networks? *Advances in Neural Information Processing Systems*
405 (Montreal), 3320–3328 (2014).
- 406 8. Mohanty, S. P., Hughes, D. P., & Salathé, M. Using deep learning for image-based
407 plant disease detection. *Frontiers in Plant Science*, 7, 1419. doi:
408 10.3389/fpls.2016.01419 (2016).
- 409 9. Ramcharan, A., Baranowski, K., McCloskey, P., Ahamed, B., Legg, J., & Hughes,
410 D. Deep learning for image-based cassava disease detection. *Frontiers in Plant
411 Science*, 8, 1852 (2017).

- 412 10. Carranza-Rojas, J., Goeau, H., Bonnet, P., Mata-Montero, E., & Joly, A. Going
413 deeper in the automated identification of Herbarium specimens. *BMC Evolutionary*
414 *Biology*, 17, 181 (2017).
- 415 11. Nogueira, K., Penatti, O. A. B., & Dos Santos, J. A. Towards better exploiting
416 convolutional neural networks for remote sensing scene classification. *Pattern*
417 *Recognition*, 61, 539–556 (2017).
- 418 12. Zhu, X.X., Tuia, D., Mou, L., Xia, G.S., Zhang, L., & Xu, F. Deep Learning in
419 Remote Sensing: A Comprehensive Review and List of Resources. *IEEE Geosci.*
420 *Remote Sens. Mag*, 5, 8–36 (2017).
- 421 13. Guirado, E., Tabik, S., Alcaraz-Segura, D., Cabello, J., & Herrera, F. Deep-learning
422 Versus OBIA for Scattered Shrub Detection with Google Earth Imagery: Ziziphus
423 lotus as Case Study. *Remote Sensing*, 9, 1220. doi: 10.3390/rs9121220 (2017).
- 424 14. Ise, T., Minagawa, M., & Onishi, M. Classifying 3 moss species by deep learning,
425 using the “chopped picture” method. *Open Journal of Ecology*, 8, 166–173 (2018).
- 426 15. Nakashima, A. The present situation of the bamboo forests management in the
427 suburbs: A case study of the bamboo shoot producing districts in the suburbs of
428 Kyoto City. *Applied Forest Science*, 10, 1–7 (in Japanese with English abstract)
429 (2001).
- 430 16. Nishikawa, R., Murakami, T., Yoshida, S., Mitsuda, Y., Nagashima, K., & Mizoue,
431 N. Characteristic of temporal range shifts of bamboo stands according to adjacent
432 landcover type. *Journal of the Japanese Forestry Society*, 87, 402–409 (in Japanese
433 with English abstract) (2005).

- 434 17. Okutomi, K., Shinoda, S., & Fukuda, H. Causal analysis of the invasion of broad-
435 leaved forest by bamboo in Japan. *Journal of Vegetation Science*, 7, 723–728
436 (1996).
- 437 18. Suzuki, S. Chronological location analyses of giant bamboo (*Phyllostachys*
438 *pubescens*) groves and their invasive expansion in a satoyama landscape area,
439 western Japan. *Plant Species Biology*, 30, 63–71 (2015).
- 440 19. NVIDIA NVIDIA deep learning gpu training system.
441 <https://developer.nvidia.com/digits>. Accessed June 1, 2018 (2016).
- 442 20. LeCun, Y. L., Bottou, L., Bengio, Y., & Haffner, P. Gradient-based learning applied
443 to document recognition. *Proceedings of the IEEE*, 86, 2278–2324. doi:
444 10.1109/5.726791 (1998).
- 445 21. Wäldchen, J., Rzanny, M., Seeland, M., & Mäder, P. Automated plant species
446 identification—Trends and future directions. *PLoS Computational Biology*, 14(4),
447 e1005993. <https://doi.org/10.1371/journal.pcbi.1005993> (2018).
- 448 22. Wäldchen, J., & Mäder, P. Machine learning for image based species identification.
449 *Methods Ecol Evol*. 2018, 1–10. doi: 10.1111/2041-210X.13075 (2018).
- 450 23. Rocchini, D., Foody, G. M., Nagendra, H. et al. Uncertainty in ecosystem mapping
451 by remote sensing. *Computers and Geosciences*, 50, 128–135 (2013).
- 452 24. Albert, A., Kaur, J., & Gonzalez, M. Using convolutional networks and satellite
453 imagery to identify patterns in urban environments at a large scale. *arXiv preprint*,
454 arXiv:1704.02965 (2017).
- 455 25. Someya, T., Takemura, S., Miyamoto, S., & Kamada, M. Predictions of bamboo
456 forest distribution and associated environmental factors using natural environmental

- 457 information GIS and digital national land information in Japan. *Keikanseitaigaku*
458 [Landscape Ecology], 15, 41–54 (in Japanese with English abstract) (2010).
- 459 26. Takano, K. T., Hibino, K., Numata, A., Oguro, M., Aiba, M., Shiogama, H.,
460 Takayasu, I., & Nakashizuka, T. Detecting latitudinal and altitudinal expansion of
461 invasive bamboo *Phyllostachys edulis* and *Phyllostachys bambusoides* (Poaceae) in
462 Japan to project potential habitats under 1.5°C–4.0°C global warming. *Ecology and*
463 *Evolution*, 7, 9848–9859 (2017).
- 464 27. Jones, H. G., & Vaughan, R. A. *Remote Sensing of Vegetation: Principles*
465 *Techniques and Applications* (Oxford University Press, 2010).
- 466
- 467
- 468
- 469
- 470
- 471
- 472
- 473
- 474